# Pressure Dependence of the Low-Frequency de Haas–van Alphen Oscillations in Zn†

W. J. O'Sullivan and J. E. Schirber
*Sandia Laboratory, Albuquerque, New Mexico*
(Received 20 June 1966)

We report the results of measurements of the pressure dependence (to ~4 kbar) of the de Haas–van Alphen (dHvA) oscillations associated with three sections of the Zn Fermi surface. For **H** along the hexad axis, the cross-sectional area of the 3rd-band electron pockets ("needles") *increases* with an initial rate given by $d\ln S_1/dP = (32\pm1.5)\times10^{-2}$ kbar$)^{-1}$. The cyclotron effective mass of the needles is also an increasing function of pressure, with a slope given by $d\ln m_1^*/dP = (14\pm2)\times10^{-2}$ kbar$^{-1}$. The minimum cross-sectional area of the waists of the combined 1st- and 2nd-band hole surface ("monster") *increases* at a rate given by $d\ln S_2/dP = (3.94\pm0.10)\times10^{-2}$ kbar$^{-1}$ and the cross-sectional area of the diagonal arms of the monster *decreases* at a rate given by $d\ln S_3/dP = -(1.27\pm0.07)\times10^{-2}$ kbar$^{-1}$. These experimental data are compared with the results of previous studies of the Fermi surface of Zn as a function of pressure and with the results of recent measurements of the effects of alloying upon the Zn Fermi surface. In addition, these results are compared with predictions of the nearly-free-electron model (NFEM), and in the case of the waist orbits a comparison is also made with the pressure behavior predicted by a screened point-ion-model pseudopotential. We conclude that previous reported results for the pressure dependence of the dHvA periods and $m^*$ for the needles in Zn are incorrect. The NFEM predictions are at least in qualitative agreement with experiment in the three cases studied. For the needles, the relation between the pressure and alloy results is in excellent agreement with the NFEM, and the observed $d\ln m^*/dP$ agrees with the predicted NFEM behavior to within experimental uncertainty. In the case of the waist orbits, the agreement between the alloy results and the model predictions seems to be significantly poorer than for the pressure results.

## I. INTRODUCTION

THE nearly free electron model[1–5] (NFEM)[6] with modifications to account for the effects of magnetic breakdown[7] and spin-orbit coupling,[8,9] has been shown to give a surprisingly quantitative description of much of the Fermi surface (FS) of zinc. (The sections of the NFEM FS of Zn relevant to the subsequent discussion are shown in Fig. 1.) Since this model relates the FS dimensions to the lattice dimensions in a uniquely defined manner, studies of the changes in the FS with hydrostatic pressure provide a sensitive test of the degree to which the NFEM can be applied to Zn.

Several investigations of the pressure dependence of the Zn FS have been carried out. Torque de Haas–van Alphen (dHvA) measurements[10,11] of the variation of the cross sectional area of the 3rd zone electron pockets ("needles") with pressure led to a change opposite in sign to the NFEM prediction. The cyclotron effective mass of the needles was also observed[10] to vary in a way not describable by the model. Measurements of the pressure dependence of the period of the magnetoresistance oscillations[12] associated with the needles gave an effect of the correct sign, but a factor of nearly three smaller than had been determined from pressure studies[13] of the Ettinghausen-Nernst effect. In addition it was inferred[12] from the pressure variation of the lengths of the angular regions supporting open orbits that the waists of the 2nd zone hole surface (the "monster," see Fig. 1) tended to pinch off with increas-

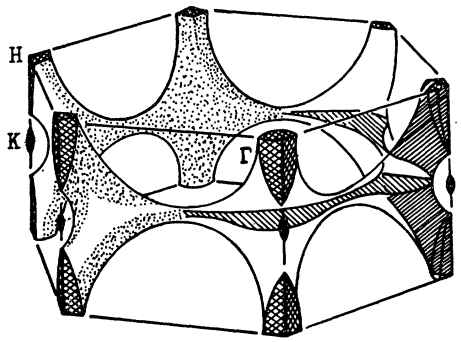


FIG. 1. First- and second-zone hole surface ("monster") and third-zone electron surfaces ("needles") of the 1-OPW Fermi surface of Zn (Ref. 4). The needles are the solid shaded ellipsoids about the point $K$. The dHvA oscillations studied in this work correspond to: (1) an orbit about the extremal cross section of the needles for **H** along the hexad axis of the zone; (2) an orbit about the minimum extremal cross section of the waists of the monster; (3) an orbit about the diagonal arms of the monster.

† This work was supported by the U. S. Atomic Energy Commission.

[1] A. S. Joseph and W. L. Gordon, Phys. Rev. **126**, 489 (1962).
[2] W. A. Harrison, Phys. Rev. **126**, 497 (1962).
[3] W. A. Harrison, Phys. Rev. **129**, 2512 (1963).
[4] W. A. Reed and G. F. Brennert, Phys. Rev. **130**, 565 (1963).
[5] R. J. Higgins, J. A. Marcus, and D. H. Whitmore, Phys. Rev. **137**, A1172 (1965).
[6] The terms NFEM and 1-OPW approximation are used synonymously to designate the free-electron model with appropriate connectivity modifications at the Bragg reflection planes.
[7] M. H. Cohen and L. M. Falicov, Phys. Rev. Letters **7**, 231 (1961).
[8] M. H. Cohen and L. M. Falicov, Phys. Rev. Letters **5**, 544 (1960).
[9] L. M. Falicov and M. H. Cohen, Phys. Rev. **130**, 92 (1963).
[10] I. M. Dmitrenko, B. I. Verkin, and B. G. Lazarev, Zh. Eksperim. i Teor. Fiz. **35**, 328 (1958) [English transl.: Soviet Phys.—JETP **8**, 229 (1959)].
[11] B. I. Verkin and I. M. Dmitrenko, Dokl. Akad. Nauk. SSSR **124**, 557 (1959) [English transl.: Soviet Phys.—Doklady **4**, 118 (1959)].
[12] Yu. P. Gaidukov and E. S. Itskevich, Zh. Eksperim. i Teor. Fiz. **45**, 71 (1963) [English transl.: Soviet Phys.—JETP **18**, 51 (1964)].
[13] K. S. Balain, C. G. Grenier, and J. M. Reynolds, Phys. Rev. **119**, 935 (1960).

ing pressure. This observation was also in opposition to the NFEM prediction. Subsequent magnetoresistance studies under pressure led[14] to results in agreement with the Ettinghausen-Nernst effect observations for the needles and implied an increase in the thickness of the waists in qualitative agreement with the NFEM.

In a recent torque dHvA study,[15] the variations of the cross sectional areas of several sections of the Zn FS with solute concentration have been measured in dilute Zn-Cu and Zn-Al alloys. These data indicated at least a qualitative agreement between the NFEM predictions and the observed results in the case of the needles, but, while correctly predicting the sign, the model greatly underestimated the magnitude of the effects of alloying upon the waists of the 2nd zone hole surface. In the process of alloying, both the lattice dimensions as well as the effective valence are changed, while only the lattice dimensions are varied in a pressure experiment. Comparison of the alloy results with related pressure-effect measurements are therefore of interest since the two measurements are complementary.

This paper reports the results of a study of the pressure variation to 4 kbar of the periods of the three lowest frequency dHvA oscillations observed in Zn. In the case of the lowest frequency oscillation the pressure dependence of the cyclotron effective mass has also been measured. The oscillations investigated and the sections of the FS with which they are associated are (see Fig. 1): (1) the needles, the 3rd-zone pockets of electrons about the point $K$ of the Zn Brillouin zone (BZ), labeled $P_1$ by Joseph and Gordon[1]; (2) the oscillations labeled[1] $P_2$ corresponding to orbits about the waists of the 2nd-zone hole surface; (3) the oscillations labeled[1] $P_3$ corresponding to orbits about the diagonal arms of the combined 1st- and 2nd-band hole surface. (While the pressure dependence of the $P_1$ dHvA oscillations has been measured, the results of this earlier work are spurious and it is important that correct values for the pressure effect on $P_1$ be determined.) By combining the measured pressure variation of the dHvA periods with the fundamental dHvA relation[16]

$$P_i = 2\pi e/\hbar c S_i, \tag{1}$$

the pressure variation of extremal cross-sectional areas ($S_i$) of the FS can be determined and compared with model predictions.

In Sec. II we discuss the experimental procedures involved in this work. In Sec. III, the results of pressure studies of the $P_1$ dHvA oscillations are given. These results are compared with model predictions and with the alloy results. Sections IV and V deal in a similar way with the $P_2$ and $P_3$ oscillations, respectively. Section VI consists of a summary of the results and conclusions. The question of the resistive and magnetic contributions to the dHvA signal in the field-modulation technique is examined in the limit of low modulation frequencies in an appendix.

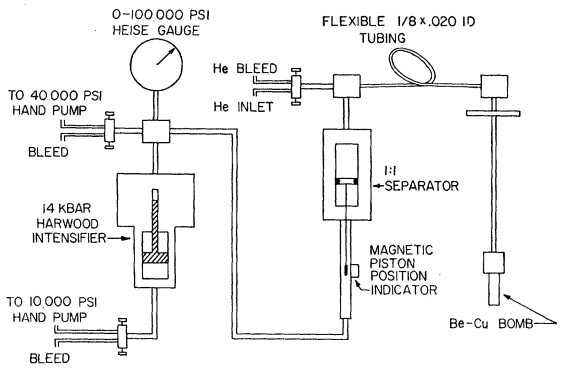


FIG. 2. Schematic of the 5 kbar solid helium pressure system (components are not drawn to scale). Kerosene is used as the pressure transmitting fluid on both sides of the intensifier.

## II. EXPERIMENTAL TECHNIQUES

The crystals used in this work were grown from 6–9's pure Zn from Cominco by zone refining in a He-gas atmosphere.[14,17] The samples (2 mm×2 mm×15 mm) were cut by acid erosion from ingots oriented by standard back reflection x-ray techniques to within 1 degree of the desired orientation. The resistance ratio of the samples (the ratio of the room-temperature resistance to that at 4°K) was about $10^4$.

The pressures were generated in solid helium. The method[14] consists of application of pressure in gaseous helium at a temperature just above the freezing point of helium at the desired pressure. This pressure is maintained at a constant value as the Be-Cu bomb ($\frac{1}{8}$ in. i.d., $\frac{7}{16}$ in. o.d.) is slowly cooled from the bottom up by lowering it into the cryostat. The temperature of the bomb is monitored during this process by a copper-constantan thermocouple. The pressure is measured on the high side of the intensifier (see Fig. 2) so that neither the intensifier ratio nor the pressure dependence of the intensifier ratio need be known. The final pressure is calculated from the phase diagram[18] of solid helium assuming that the cooling from the freezing point is at constant volume. The absolute error in the value of the pressure is estimated to be less than 5% but pressures can be reproduced to within 1% with this method. Since the pressure transmitting medium is solid He, it is necessary to raise the bomb out of the cryostat to allow the helium to melt before the pressure can be varied. In order to prevent motion of the sample during these pressure changes, the samples were slip-fit into copper-wire helices which made close contact with the inner walls of the bomb. In addition, the measurements were usually made for the magnetic field along, or

[14] J. E. Schirber, Phys. Rev. **140**, A2065 (1965).
[15] R. J. Higgins and J. A. Marcus, Phys. Rev. **141**, 553 (1966).
[16] L. Onsager, Phil. Mag. **43**, 1006 (1952).
[17] R. W. Stark, Phys. Rev. **135**, A1698 (1964).
[18] J. S. Dugdale, in *Physics of High Pressures in the Condensed State*, edited by A. van Itterbeek (North-Holland Publishing Company, Amsterdam, 1965).

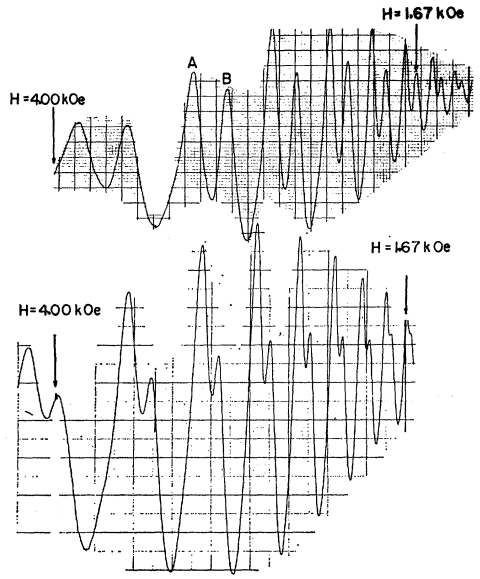


FIG. 3. Reproductions of two samples of the needle dHvA oscillations in Zn for $\mathbf{H}\|b_3$ and $T=1.2$°K. The upper trace was taken at $P\cong 1$ bar and the lower trace was taken at $P=1.17$ kbar. These data were detected at the 2nd harmonic of the modulation frequency ($\omega/2\pi=200$ cps).

close to, directions where the dHvA periods vary slowly with orientation.

The conventional field modulation technique introduced by Shoenberg and Stiles[19] was used for this work. Standard phase-sensitive detection methods were used to process the fundamental and 2nd harmonic[20] signal components. The modulation frequencies used varied from 6.25 to 3600 cps. However, most of the data were taken with a modulation frequency of 6.25, 50, or 200 cps. The slowly varying magnetic field component was produced by a high homogeneity 55 kOe superconducting solenoid. The modulation coil (5 in. long No. 40 A.W.G. copper wire) was wound inside the vacuum space of the tail of the helium-Dewar insert. The pickup coil was made up of two coils wound in series opposition on a common phenolic form which slip-fit over the Be-Cu bomb. Each half of the pickup coil consisted of about 3000 turns of No. 46 A.W.G. copper wire. The field-versus-current calibration provided with the magnet was used to determine the magnetic field values throughout this work. This calibration was shown to be good to about 0.5% by comparing dHvA period values in Zn and Pb with the results of other investigators.[1,21] The modulation field amplitude-versus-current calibration was determined to within a few percent by measuring the applied field values at which the zeroes[22] of $J_2(2\pi rFH_m/H^2)$ occurred in the 2nd-harmonic dHvA signal associated with the majority electron pockets in graphite (this metal provided a dHvA frequency $F$ in a convenient range).

[19] D. Shoenberg and P. J. Stiles, Proc. Roy. Soc. (London) A281, 62 (1964).

[20] The term dHvA harmonic will be used when referring to the harmonics in $(1/H)$, to distinguish these from the harmonics of the modulation frequency.

[21] J. R. Anderson and A. V. Gold, Phys. Rev. 139, A1459 (1965).

[22] A. Goldstein, S. J. Williamson, and S. Foner, Rev. Sci. Instr. 36, 1356 (1965); and S. J. Williamson, thesis, Massachusetts Institute of Technology, 1965 (unpublished). These references discuss the ac-modulation technique in some detail.

## III. EFFECT OF PRESSURE UPON THE NEEDLE dHvA OSCILLATIONS ($P_1$)

### A. Pressure Dependence of the Period

The variation of the extremal cross sectional area of the needle electron pockets in Zn was measured to pressures of 4 kbar. Field orientations studied were[23]: $\mathbf{H}\|b_3$, $\mathbf{H}$ at 20° to $b_3$ in $(10\bar{1}0)$, and $\mathbf{H}$ at 20° to $b_3$ in $(11\bar{2}0)$. Recorder tracings[24,25] of the needle oscillations taken at two different pressures are shown in Fig. 3.

We find that the cross sectional area of the needles increases rapidly with pressure at an initial rate given by[26]

$$d\ln S_1/dP=(32.0\pm 1.5)\times 10^{-2}\ (\text{kbar})^{-1} \qquad (2)$$

for $H\|b_3$. [The rate of increase for $H$ at 20° to $b_3$ is $(30.0\pm 1.5)\times 10^{-2}$ (kbar)$^{-1}$; i.e., it is unchanged within experimental uncertainty.] Thus, the minimum extremal area of the needles doubles with the application of about 3 kbar of hydrostatic pressure. The error estimate in the above pressure derivative reflects the uncertainty in the actual value of the pressure, rather than the uncertainty in the determination of the period change. In Fig. 4 we show a plot of our results for $[S_1(P)-S_1(0)]/S_1(0)$ as a function of the $c/a$ ratio[27] for $\mathbf{H}\|b_3$. (The variation of the $c/a$ ratio with pressure was calculated using the linear compressibilities determined by Alers and Neighbours[28] from measurements of the elastic constants of Zn at 4.2°K.) For comparison, we have plotted the results of several other measurements of the needle cross sectional area with changes in the $c/a$ ratio. These are: (1) the torque measurements by Berlincourt and Steele[29] of the period of the needle

[23] The reciprocal lattice vectors in the basal plane of the hexagonal unit cell are labeled $b_1$ and $b_2$, and $b_3$ is the lattice vector along the hexad axis.

[24] Each of the two subpeaks of a given oscillation corresponds to the contribution from one half of a spin split Landau level and has the same significance as that attached by Stark (Ref. 17) to the spin sublevels he observed in the oscillatory Hall conductivity in Zn. That is, the separation in $(1/H)$ between these subpeaks is directly related to the Zeeman energy difference between the two spin states associated with each Landau level. The pressure dependence of the spin splitting of the needle Landau levels and its relation to the $g$ factor of the needles has been discussed in a previous publication (Ref. 25).

[25] W. J. O'Sullivan and J. E. Schirber, Phys. Rev. Letters 16, 691 (1966); and to be published.

[26] The preliminary results of the pressure variation of $P_1$ were first published in W. J. O'Sullivan and J. E. Schirber, Phys. Letters 18, 212 (1965). The derivatives of the form $d\ln S/dP$ are defined as $d\ln S/dP\equiv[1/S(0)][S(P)-S(0)]/P$.

[27] We assume that $c/a=1.8300$ at 4.2°K.

[28] G. A. Alers and J. R. Neighbours, J. Phys. Chem. Solids 7, 58 (1958).

[29] T. G. Berlincourt and M. C. Steele, Phys. Rev. 95, 1421 (1954).

dHvA oscillations as a function of temperature ($P\cong 1$ bar); (2) Schirber's results[14] for the pressure dependence of the oscillations in the transverse magnetoresistance, $(\Delta\rho_{11}/\rho_0)_{osc}$, where the method of isobaric freezing of solid He was used to generate the pressure about the sample; (3) the results of Gaidukov and Itskevich[12] for the pressure dependence of the period of $(\Delta\rho_{11}/\rho_0)_{osc}$, where the frozen oil–kerosene method was used to generate the pressure; (4) the torque dHvA results of Dmitrenko, Verkin, and Lazarev[10] who used the ice bomb technique to generate the pressure.

Our results are in excellent agreement with the solid-He pressure measurements[14] on $(\Delta\rho_{11}/\rho_0)_{osc}$. Further, the value we determine for $d\ln S_1/dP$ is in agreement with that determined by Balain, Grenier, and Reynolds.[13] These investigators found an initial slope for $\Delta S_1/S_1(0)$ of $(32\pm 6)\times 10^{-2}$ (kbar)$^{-1}$ from measurements of the oscillatory behavior of the Ettinghausen-Nernst effect under purely hydrostatic conditions in fluid He. We also observe that, within their experimental uncertainty, our data is a continuation to smaller $c/a$ values of the data of Berlincourt and Steele.[29] From these comparisons we conclude that the method of isobaric freezing of solid He assures hydrostatic conditions even when applied to a material with highly anisotropic thermal expansion coefficients, such as Zn. As an additional test of this conclusion, we determined the pressure variation of the needle cross-sectional area using the phase shift technique of Shoenberg and Stiles[19] and of Templeton.[30] These measurements were carried out at 4.0°K and with He *fluid* pressures of up to 1800 psi. The $(1/H)$ values corresponding to a given feature of two different needle oscillations were measured at atmospheric pressure. Then the pressure was changed by pumping on He gas and the shifted $(1/H)$ values recorded. The pressure derivative of the cross sectional area was determined from the relation,

$$d\ln S/dP=-\frac{F(0)}{n_1-n_2}\frac{d}{dP}\{(1/H)_1-(1/H)_2\}, \quad (3)$$

where $F(0)$ is the frequency at atmospheric pressure and $n_1$ and $n_2$ are the numerical indices of the two oscillations involved. The resultant value is $d\ln S_1/dP=(30\pm 3)\times 10^{-2}$ (kbar)$^{-1}$. In this measurement the pressure uncertainty was negligible. The relatively large error in the result followed from a combination of the $\sim$6 Oe scatter in our field readings and the low numerical index of the oscillations. (The largest value of $n$ used was 11. The effect of trapped flux in the solenoid becomes important for larger $n$ values.) Nevertheless, the result agrees with the value determined using the frozen-He technique.

Gaidukov and Itskevich[12] determined an initial slope given by $d\ln S_1/dP=(12\pm 3)\times 10^{-2}$ (kbar)$^{-1}$. We conclude that their pressure transmitting medium does not flow sufficiently in the low pressure regime (up to 7 kbar) to assure hydrostatic conditions. If the pressure medium does not flow easily, the "pressure" experienced by a sample with anisotropic thermal expansion coefficients may be quite different than that registered by independent internal pressure calibrations such as the superconducting transition temperature of Sn used by Gaidukov and Itskevich. In later work, Itskevich, Voronovskii, and Sukhoparov[31] have extended the pressure measurements on $(\Delta\rho_{11}/\rho_0)_{osc}$ in Zn to 15 kbar. These more recent results seem to indicate that at higher pressures the frozen kerosene-oil medium deforms more easily. Since $\Delta S_1/S_1(0)$ is a nonlinear function of pressure, it is not possible to extrapolate our data to higher pressures to check this supposition.

The results of the torque dHvA ice bomb measurements of Dmitrenko, Verkin, and Lazarev[10] clearly suffer from the extreme resistance to flow of the pressure medium. Their conclusions that the needle surfaces

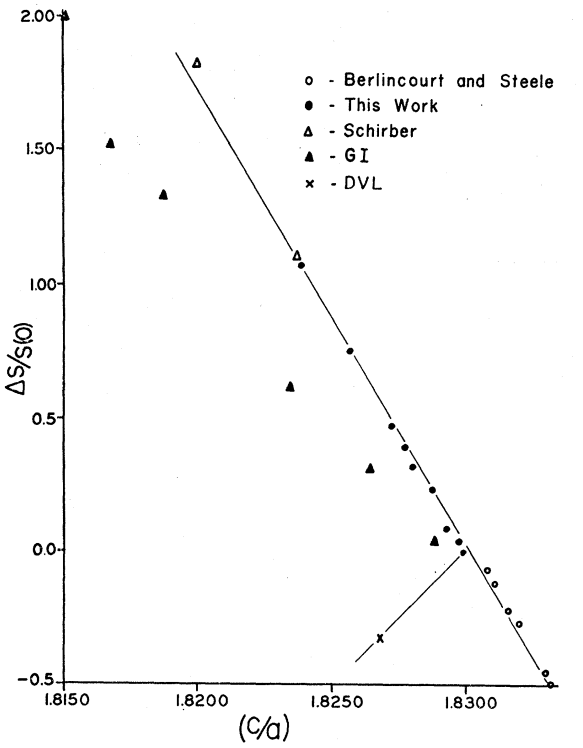


FIG. 4. A plot of our results (shaded circles) for $\Delta S/S(0)$ for the needles as a function of the $c/a$ ratio. In addition, we include: (1) the results of the measurements of Berlincourt and Steele (open circles) of the temperature dependence of the needle cross sectional area; (2) the pressure dependence of the needle area determined by Gaidukov and Itskevich (shaded triangles) from $(\Delta\rho_{11}/\rho_0)_{osc}$; (3) the pressure dependence of the needle area determined by Schirber (open triangles) from $(\Delta\rho_{11}/\rho_0)_{osc}$; (4) the pressure dependence of the needle area determined by Dmitrenko, Verkin, and Lazarev (cross) from the pressure dependence of the dHvA period.

[30] I. Templeton, Proc. Roy. Soc. (London) **292A**, 413 (1966).

[31] E. S. Itskevich, A. N. Voronovskii, and V. A. Sukhoparov, JETP Pis'mav Redaktsiyu **2**, 67 (1965) [English transl.: Soviet Phys.—JETP Letters **2**, 42 (1965)].

respond in a highly nonfree electron manner to pressure must be considered invalid. Dmitrenko and Verkin seemed to find confirmation of their ice bomb results from period measurements of the dHvA needle oscillations under a *small* uniaxial stress.[32] We conclude that their experimental uncertainty was greater than they estimated.

### B. Pressure Dependence of the Needle Effective Mass

Since the cross-sectional area of the needles in Zn is a sensitive function of pressure, the pressure variation of the cyclotron effective mass ($m^*$) of the needles should be detectable. A measurement of the pressure coefficient of $m^*$ for the needles is of interest for two reasons. Since $m^*$ is proportional to $(\partial S/\partial E)$, a value for the pressure derivative of $m^*$ provides a sensitive test of the NFEM representation of the needle surface. An *estimate* of the variation of $m^*$ with energy can be derived from the measured pressure change of $m^*$. This result is required to derive a unique value for the needle $g$ factor from the dHvA results.[25]

We determined the cyclotron effective mass and its pressure derivative from the temperature dependence of the amplitudes of the dHvA oscillations detected at the 2nd harmonic of the modulation frequency. Under conditions which are satisfied in our effective-mass measurements,[22] the total 2nd-harmonic amplitude is

$$V_2(H,T)=KT\omega(H)^{-1/2}\sum_{r=1}^{\infty} r^{-1/2}\{\exp(-\pi^2 rkT_D/\beta^* H)/\sinh(\pi^2 rkT/\beta^* H)\}\sin\left[\frac{2\pi rF}{H}-2\pi r\gamma\mp\frac{\pi}{4}\right]\times\cos(r\pi gm^*/2m_0)J_2(2\pi rFH_m/H^2). \quad (4)$$

In Eq. (4) $K$ is a constant which includes the constants appearing in the Lifshitz and Kosevich expression[33] for the oscillatory susceptibility plus terms related to the effective geometrical coupling between the sample and pickup coil, $\omega$ is the frequency of the modulation field of amplitude $H_m$, $H$ is the slowly varying component of the magnetic field, $J_2$ is the Bessel function of 2nd order and $\beta^*\equiv(eH)/(2m^*c)$. There are two sources of difficulty which tend to hinder accurate determination of the needle cyclotron effective mass. First, because of the small Dingle temperature (our measured $T_D$ values are about 0.5°K) and small $m^*$ ($m^*\cong 0.0075m_0$ for $H\|b_3$) coupled with the dHvA harmonic enhancement intrinsic in the ac detection method, the dHvA harmonic content of the oscillations remains high except at low fields ($H<1$ kOe) or at high temperatures ($T>4.0$°K). Second, because of the small $m^*$, the variation of the signal amplitude with temperature is weak for fields much above 1 kOe. These problems were easily avoided by measuring the amplitude temperature dependence within the field range 0.5 kOe–0.9 kOe, and within the temperature range 1.5–4.0°K. Under these conditions, $V_2(H,T)$ is dominated by the first dHvA harmonic contribution and $m^*$ can be determined from a plot of

$$\ln[V_2(H,T)\exp(\pi^2 kT/\beta^* H)/2T\sinh(\pi^2 kT/\beta^* H)] \text{ versus } T.$$

The values for $m_1^*$ at $P\cong 1$ bar are in excellent agreement with those quoted by Joseph and Gordon. We find $m_1^*(0)=(0.0075\pm 0.0005)m_0(H\|b_3)$ and $m_1^*(0)=(0.0084\pm 0.0005)m_0$ ($H$ at 20° to $b_3$). The effective mass was measured to 4 kbar and the logarithmic pressure derivative of $m_1^*$ is,

$$d\ln m_1^*/dP=(14\pm 2)\times 10^{-2}\ (\text{kbar})^{-1}. \quad (5)$$

No significant difference was detected between the results for $H\|b_3$ and $H$ at 20° to $b_3$. The quoted errors reflect the scatter of $m_1^*$ determinations among 6 different oscillations within the selected field range and among several runs at each pressure.

### C. Comparison of the Needle-Pressure Results with the NFEM and with the Results of Alloy Studies

Since the pseudopotential form factor $W(100)$ contributing to Bragg scattering in the region of the point $K$ of the hcp BZ (see Fig. 1) is very small in Zn, the needles should be describable in terms of the one-orthogonalized-plane-wave (1-OPW) approximation.

The needle extremal area for $H\|b_3$ is given in the 1-OPW approximation by [34,35]

$$S_1(\text{NFEM})=\frac{4\pi}{9}\left(\frac{2\pi}{a}\right)^2\left[\left(\frac{\beta Z}{c/a}\right)^{1/3}-1\right]^2, \quad (6)$$

where $\beta\equiv 27\sqrt{3}/16\pi$.

The predicted pressure derivative for the needle area is

$$\frac{d\ln S_1(\text{NFEM})}{dP}=-\left[2\frac{d\ln a}{dP}+\frac{\frac{2}{3}(\beta Z/(c/a))^{1/3}}{[(\beta Z/(c/a))^{1/3}-1]}\left(\frac{d\ln(c/a)}{dP}\right)\right]. \quad (7)$$

The first term within the brackets contributes about 2% of the total pressure coefficient and will be neglected. In this approximation, the pressure coefficient is a function only of $\rho(\rho=Z/(c/a))$ and the pressure derivative

[32] B. I. Verkin and I. M. Dmitrenko, Zh. Eksperim. i Teor. Fiz. **35**, 291 (1958) [English transl.: Soviet Phys.—JETP **8**, 200 (1959)].

[33] I. M. Lifshitz and A. M. Kosevich, Zh. Eksperim. i Teor. Fiz. **29**, 730 (1955) [English transl.: Soviet Phys.—JETP **2**, 635 (1956)].

[34] W. A. Harrison, Phys. Rev. **118**, 1190 (1960).

[35] This is the form given by Higgins and Marcus (Ref. 15) rather than by Harrison (Ref. 34). Both expressions for $S_1$ lead to the same predicted pressure behavior.

of the $c/a$ ratio.[28] For $Z=2$ and $c/a=1.8300$,

$$\frac{d\ln S_1(\text{NFEM})}{dP}\cong 13\times 10^{-2}\ (\text{kbar})^{-1}, \qquad (8)$$

or less than half of the observed effect. This direct comparison between the 1-OPW theory and experiment has little significance because of the *extreme* sensitivity of the result to small variations in the initial $c/a$ value. (The NFEM value for $S_1$ is about a factor of two greater than the experimental value. Reduction of the model area results in a greater value for $d\ln S_1/dP$.) Stronger support for the 1-OPW character of the needles can be derived from a comparison between the pressure and alloying effects upon the period of the needles and between the pressure dependence of $m^*$ and the predicted 1-OPW behavior.

The form of the 1-OPW expressions [Eq. (6)] requires that

$$\frac{\partial \ln S_1}{\partial \ln \rho}=-\left(\frac{\partial \ln S_1}{\partial \ln (c/a)}\right)_Z, \qquad (9)$$

when the approximation discussed previously is invoked. From their measurements of the needle cross-sectional area in dilute Zn-Cu alloys, Higgins and Marcus[15] determined $\partial \ln S_1/\partial \ln\rho\cong 2.70\times 10^2$, which is in excellent agreement with our value of $[\partial \ln S_1/\partial \ln(c/a)]_Z = -2.78\times 10^2$.

From Eq. (6), the needle effective mass[36] is proportional to $(S_1)^{1/2}$ and therefore the NFEM predicts that $m_1^*$ changes with pressure at half the rate of change of $S_1$. The NFEM prediction for the pressure change of $m_1^*$ is,

$$\frac{d\ln m_1^*(\text{NFEM})}{dP}=\frac{1}{2}\frac{d\ln S_1}{dP}=16\times 10^{-2}\ (\text{kbar})^{-1}, \qquad (10)$$

where we have used the experimental value for $d\ln S_1/dP$. The measured pressure coefficient of $m^*$ is $14\times 10^{-2}$ (kbar)$^{-1}$, in good agreement with the model prediction. [This latter result is also consistent with the $m^*$ observations of Higgins and Marcus who observed no change in $m^*$ greater than their $\pm 10\%$ uncertainty for up to 0.21% Cu in Zn, where $\Delta S_1/S_1$ (pure Zn)$\cong$30% for 0.21% Zn-Cu.]

We conclude that the 1-OPW model offers a semiquantitatively correct description of the needle behavior under changes in lattice dimension and valence.

### D. Oscillatory Magnetoresistance Contributions to the Needle dHvA Signal

In addition to the magnetic-susceptibility oscillations associated with the needles in Zn, there are also large amplitude oscillations in the magnetoresistance.[17] In an appendix to this paper we show that for 1st-harmonic (fundamental) detection and for low modulation frequency and small modulation amplitude, the oscillatory component of the signal is solely due to the magnetization oscillations. Although a complete 2nd-harmonic solution was not carried out it is apparent from inspection that important contributions can be expected from $(\Delta\rho/\rho_0)_{\text{osc}}$ to the second-harmonic component of the signal.

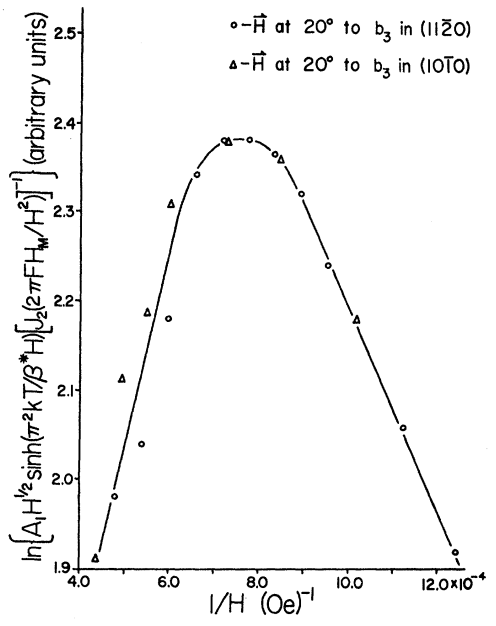


FIG. 5. Amplitude plots of the needle dHvA oscillations (2nd harmonic detection) for $H$ at 20° to $b_3$ in (11$\bar{2}$0) and in (10$\bar{1}$0).

Recently Gaidukov and Krechetova[37] have shown that the amplitude of the oscillations in the transverse magnetoresistance is correlated with the regions of field orientation which support open orbits in Zn. They found that large amplitude oscillations in $(\Delta\rho_{11}/\rho_0)_{\text{osc}}$ appeared when the applied field lay within an open-orbit "whisker" and were not observable outside of the open-orbit regions.

If there is a large resistive contribution to the needle signal when detected at the 2nd harmonic of the modulation frequency, we would expect this to be manifested in the amplitude–versus–applied-field characteristics of the data for field orientations within and outside open orbit regions. (This conclusion is based upon the *assumption* that the amplitude–versus–field characteristics of the susceptibility and magnetoresistance oscillations differ.) To investigate this possibility, we studied the field dependence of the 2nd-harmonic signal amplitude at various temperatures and pressures for $H$ at 20° to $b_3$ in (11$\bar{2}$0) ($\simeq$15° outside an open orbit region) and for $H$ at 20° to $b_3$ in (10$\bar{1}$0) (about 22° inside an open

[36] R. J. Higgins, thesis, Northwestern University, 1965 (unpublished).

[37] Yu. P. Gaidukov and I. P. Krechetova, JETP Pis'mav Redaktsiyu **1**, 25 (1965) [English transl.: Soviet Phys.—JETP Letters **1**, 88 (1965)].

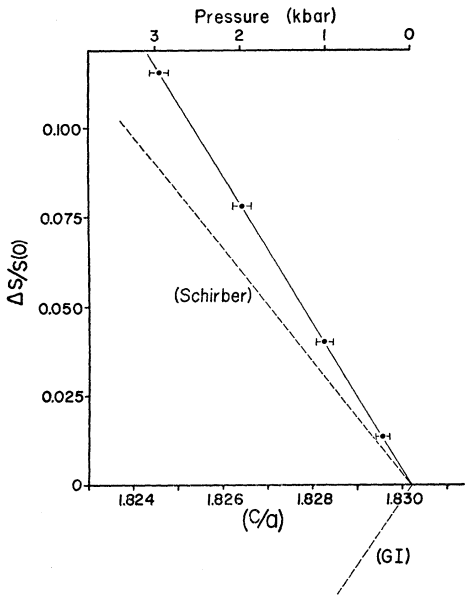


FIG. 6. Our results for the pressure dependence of the minimum extremal cross sectional area of the waists of the monster (solid circles). We have also included the pressure changes inferred by Schirber and by Gaidukov and Itskevich from magnetoresistance measurements of the pressure effect on the angular regions supporting open orbits in Zn.

orbit region). Sample Dingle plots for the two orientations are compared in Fig. 5. The characteristic reduction of the amplitude above a critical field is a result of breakdown between the needles and the monster.[9,17,38,39] In no case studied was there a detectable difference between the amplitude-versus-field characteristics for the two orientations.[40] To the extent that the assumption of a significant difference between the resistive and susceptibility-versus-field characteristics is valid, this result suggests that the 2nd-harmonic signal derives primarily from the magnetization oscillations.[41]

We also compared our amplitude-versus-field characteristics plots for $\mathbf{H}\|b_3$ and $\mathbf{H}$ at 20° to $b_3$ with similar plots of the torque dHvA data.[36,38,39] In contrast to the alloy results[36,39] in which apparent changes in the breakdown field due to enhanced impurity scattering were noted, there were no observable pressure effects on either $T_D$ or the breakdown field.

[38] J. R. Lawson and W. L. Gordon, *Proceedings of the Ninth International Conference on Low Temperature Physics* (Plenum Press, Inc., New York, 1964), Part B, p. 854.

[39] R. J. Higgins, J. A. Marcus, and D. H. Whitmore, *Proceedings of the Ninth International Conference on Low Temperature Physics* (Plenum Press, Inc., New York, 1964), Part B, p. 859.

[40] This particular comparison was made before our system for sweeping $H_m$ as $H^2$ was completed. Use of the $H_m{}^2$ sweep improved the reproducibility of our $T_D$ measurements without altering the above result.

[41] It is important to note that this comparison relates only to a part of the oscillatory resistance component in the signal. Gaidukov and Krechetova studied only $(\Delta\rho_{11}/\rho_0)_{\rm osc}$. Oscillations in the Hall resistance, $(\Delta\rho_{12}/\rho_0)_{\rm osc}$, may occur over a wider angular region.

## IV. EFFECT OF PRESSURE UPON THE WAIST dHvA OSCILLATIONS ($P_2$)

### A. Experimental Results

The waist dHvA oscillations correspond to the second longest period ($P_2$) observed by Joseph and Gordon[1] and are due to orbits about the horizontal arms of the second-zone hole surface (see Fig. 1). We have measured the pressure dependence to 4 kbar of the extremal cross-sectional area of the waists for $\mathbf{H}$ along $[11\bar{2}0]$. (With this field orientation the *minimum* extremal area of the waists of the monster is observed.) The zero-pressure period is $P_2(0)=(2.225\pm0.010\times10^{-6}\ \mathrm{G}^{-1})$ which agrees to within 2% with the period quoted by Joseph and Gordon for $\mathbf{H}$ along $[11\bar{2}0]$. Our results for the variation of the minimum extremal waist area with pressure are plotted in Fig. 6. The initial rate of change of the waist area is

$$d\ln S_2/dP=(3.94\pm0.10)\times10^{-2}\ (\mathrm{kbar})^{-1}. \quad (11)$$

That is, the waists of the monster increase with pressure at a rate which is roughly $\frac{1}{8}$ the rate of increase of the needles. We have included the results of two other experimental measurements of the waist pressure dependence in Fig. 6. From magnetoresistance studies of the pressure variation of the "lengths" of the angular regions ("whiskers") supporting open orbits in Zn, Schirber[14] inferred that the waists increased at a rate given by $d\ln S_2/dP=3\times10^{-2}\ (\mathrm{kbar})^{-1}$. From magnetoresistance measurements identical in principle to the above, Gaidukov and Itskevich[12] suggested that the connectivity in the basal plane of the Zn FS would be broken at pressures of 30 kbar. We see that the results of Schirber's magnetoresistance measurements are in good agreement with the direct dHvA determination. (The possible reasons for the spurious result of Gaidukov and Itskevich are discussed in Ref. 14.)

An attempt was made to determine a pressure shift of $m^*$ for the waists. No detectable variation of $m^*$ was observed for pressures up to 4 kbar. From the uncertainty in our effective mass measurements for the waists, we conclude that $|d\ln m_2{}^*/dP|<2\times10^{-2}\ (\mathrm{kbar})^{-1}$.

### B. Comparison of the Waist-Pressure Results with Model Predictions and with the Alloy Results

The 1-OPW area for the minimum cross section of the waists is 0.013 $(\mathrm{a.u.})^{-2}$, a factor of 10 greater than the experimentally observed area of 0.0012 $(\mathrm{a.u.})^{-2}$. The discrepancy between the 1-OPW and experimental areas is much smaller for the other sections of the FS investigated. The 1-OPW needle area [Eq. (6)] is greater than the experimental area by about a factor of two. Harrison found agreement of 10% to 50% between the 1-OPW predicted areas and the remaining areas measured by Joseph and Gordon. Therefore, band-gap effects greatly modify the waist orbits in the region of their minimum cross section. One might

expect poor agreement between the 1-OPW prediction for the pressure dependence of the waist area and the experimental result.

We carry out a calculation of the 1-OPW pressure dependence of the waist area based upon an approximate geometrical expression for the waist cross-sectional area. (This is the approximation used by Higgins and Marcus[15] and we apply their notation without change.) The approximate 1-OPW waist area for $\mathbf{H}\|[11\bar{2}0]$ is shown in Fig. 7 and is given by $(m)(h)$, where

$$m=b_3-k_F[1-((b_1/k_F)-1)^2]^{1/2}$$

and (12)

$$h=b_1-k_F\{1+[1-(b_3/k_F)^2]^{1/2}\}.$$

Since the 1-OPW area is a factor of 10 larger than the experimental area, the model prediction for $d\ln S_2/dP$ cannot be expected to compare with experiment. We are interested in determining if the increase in the waist area with pressure can be explained in terms of free-electron-like adjustments of the FS with the changes in lattice dimension. Following Higgins and Marcus we allow $k_F$ to increase by about 3% to bring the 1-OPW waist area into agreement with experiment. From Eq. (12), using the values for $b_3$ and $b_1$ at 4.2°K,[42] the adjusted $k_F$ and the experimental compressibilities,[28] we determine,

$$\frac{d\ln S_2(\text{Modified NFEM})}{dP}=2.8\times10^{-2}\ (\text{kbar})^{-1}, \quad (13)$$

a result which is in quite good agreement with the experimental value of $3.94\times10^{-2}$ (kbar)$^{-1}$. [The NFEM predicts a value for $d\ln m_2^*/dP$ of less than $2\times10^{-2}$ (kbar)$^{-1}$ which is within our estimated experimental uncertainty.] Using the same modified NFEM approximation to the waists, Higgins and Marcus determined the *initial* slopes,

$$\frac{d\ln S_2(\text{Modified NFEM})}{dC}\cong 3\times10^{-1}(1\%\ \text{Cu})^{-1}$$

$$[14\times10^{-1}(1\%\ \text{Cu})^{-1}] \quad (14)$$

and

$$\frac{d\ln S_2(\text{Modified NFEM})}{dC}\cong -2\times10^{-1}(1\%\ \text{Al})^{-1}$$

$$[-7\times10^{-1}(1\%\ \text{Al})^{-1}],$$

where $C$ is the solute concentration in atomic percent and the quantities in square brackets are their experimental results. The relatively good agreement between the 1-OPW model and the experimental pressure shift of the waist area is not reflected in the alloy results,

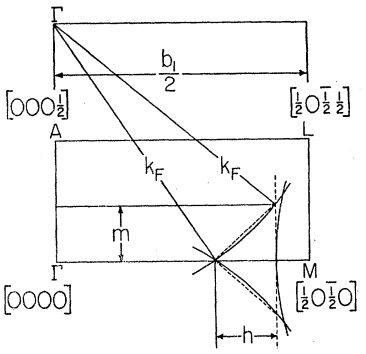


FIG. 7. The approximation used by Higgins and Marcus (triangular region) to represent the 1-OPW waist section (solid arcs) for $H$ along $[11\bar{2}0]$. The expressions for the dimensions $m$ and $h$ are given in the text.

where the model predicts changes smaller by a factor of about 4 than are observed.

Since Harrison[2] obtained an improved fit to the Zn FS with a 3-OPW model, it is of interest to determine if the relative agreement between the experimental pressure and alloy results and theory can be improved by analyzing the results in terms of the 3-OPW model.

The calculation follows the outline provided by Harrison.[2,3,43] The cross-sectional area of the waists at zero pressure and for $\mathbf{H}\|[11\bar{2}0]$ is determined using the values for the three pseudopotential form factors which Harrison found[2] gave the best fit (for only 3-OPW's) to the dHvA data of Joseph and Gordon.[1] The values for the two form factors which contribute to scattering in the region of the waists are, $W(002)=-0.0612$ Ry and $W(101)=0.0337$ Ry. [The structure factor, $S(q)$, is 1 for $q(002)$ and $\sqrt{3}/2\exp(i\varphi)$, where $\varphi=\tan^{-1}(1/\sqrt{3})$ for $q(101)$.] The variation of the waist area with pressure was calculated from the pressure variation of a model pseudopotential of the screened point-ion potential form[44] (in atomic units, a.u.),

$$W_M(q)=(-8\pi Z/q^2+\beta)(\Omega_0\epsilon(q))^{-1}. \quad (15)$$

In this expression, $Z$, the effective valence is taken to be 2 for Zn, $\Omega_0$ is the volume/atom, $\beta$ is the delta function repulsive core parameter and $\epsilon(q)$ is the static Hartree dielectric function for free electrons given (in a.u.) by,

$$\epsilon(q)=1+\frac{6\pi}{q^2}\left(\frac{Z}{\Omega_0 E_F}\right)\left\{1+\frac{(1-\eta^2)}{2\eta}\ln\left|\frac{1+\eta}{1+\eta}\right|\right\}, \quad (16)$$

with $\eta=\frac{1}{2}q/k_F$. We adjust $\beta$ so that $W(q)$ changes sign in the region of $q(100)$. This gives us a $\beta=23.8$ Ry a.u.[3] rather than $\beta=26.5$ (obtained by fitting the form factors calculated by Harrison[3]) or $\beta=24.7$ (obtained by fitting the form factors of Animalu and Heine[45]).

The model potential is plotted in Fig. 8 along with the "experimental" form factors of Harrison.[2] The two relevant model form factors are $W_M(002)=-0.0215$ Ry and $W_M(101)=0.0332$ Ry. The fit to $W(002)$ is

[42] The 4.2°K lattice parameters for Zn were obtained by combining room temperature lattice parameters from W. B. Pearson, *Lattice Spacings and the Structure of Metals and Alloys* (Pergamon Press, Inc., New York, 1958) with the thermal expansion data of R. W. Meyerhoff and J. F. Smith, J. Appl. Phys. **33**, 219 (1962).

[43] W. A. Harrison, *Physics of Solids at High Pressures* (Academic Press Inc., New York, 1965).

[44] W. A. Harrison, Phys. Rev. **131**, 2433 (1963).

[45] A. O. E. Animalu and V. Heine, Phil. Mag. **12**, 1249 (1965).

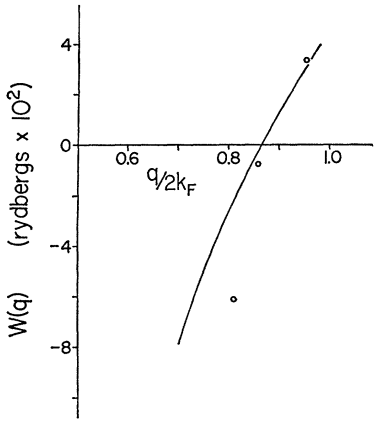


FIG. 8. The screened-ion model pseudopotential form factor, $W_M(q)$ used in the 3-OPW calculation of the pressure dependence of the waist cross sectional area. The three form factors used by Harrison to fit the dHvA data of Joseph and Gordon are included for comparison (circles).

very poor. Nevertheless, we assume that the slope $[dW_M(002)/dq]$ is an adequate representation of the slope of a better model potential in the region of $q(002)$. We find

$$\frac{1}{W_M(101)}\frac{dW_M(101)}{dP}=0.48\times10^{-2}\ (\text{kbar})^{-1},$$

and (17)

$$\frac{1}{W(002)}\frac{dW_M(002)}{dP}=-0.67\times10^{-2}\ (\text{kbar})^{-1}.$$

With the estimated pressure coefficients for the pseudopotential we determine

$$\frac{d\ \ln S_2(\text{3-OPW})}{dP}=2.2\times10^{-2}\ (\text{kbar})^{-1}. \quad (18)$$

While this result agrees to within a factor of 2 with experiment, the assumption made in estimating the pressure change of $W(002)$ is probably as questionable as the approximation involved in increasing $k_F$ to fit the experimental area in the NFEM calculation.

The model pseudopotential calculation was also extended to calculate the 3-OPW predictions for the change in the waist area due to alloying. Applying the values used by Higgins and Marcus for the variation of the Zn lattice parameters with solute concentration, we find the *initial* slopes

$$\frac{1}{W_M(101)}\frac{dW_M(101)}{dC}\cong3\times10^{-2}(1\%\ \text{Cu})^{-1}$$

and (19)

$$\frac{1}{W(002)}\frac{dW_M(002)}{dC}\cong-7\times10^{-2}(1\%\ \text{Cu})^{-1},$$

for the Zn-Cu alloy system and

$$\frac{1}{W_M(101)}\frac{dW_M(101)}{dC}\cong-2\times10^{-2}(1\%\ \text{Al})^{-1},$$

and (20)

$$\frac{1}{W(002)}\frac{dW_M(002)}{dC}\cong3\times10^{-2}(1\%\ \text{Al})^{-1},$$

for the Zn-Al alloy system. The area changes based on the initial slopes are,

$$\frac{d\ \ln S_2(\text{3-OPW})}{dC}\cong4\times10^{-1}(1\%\ \text{Cu})^{-1}$$

and (21)

$$\frac{d\ \ln S_2(\text{3-OPW})}{dC}\cong-1\times10^{-1}(1\%\ \text{Al})^{-1},$$

in contrast with the experimental results ($d\ \ln S_2/dC=14\times10^{-1}$ (1% Cu)$^{-1}$ and $d\ \ln S_2/dC=-7\times10^{-1}$ (1% Al)$^{-1}$.

The discrepancy between theory and the experimental alloying results for the waists is not reduced, and the difference between the degree of agreement of the pressure and alloying experimental results with the model predictions seems to be significant. This is to be contrasted with the excellent correspondence between the pressure and alloy results on the needles.

## V. PRESSURE DEPENDENCE OF THE DIAGONAL-ARM ORBITS ($P_3$)

### A. Experimental Results

This orbit corresponds to the third longest period ($P_3$) studied by Joseph and Gordon[1] and has been assigned by Harrison[2] to an orbit which circumscribes a section of both the second-band diagonal arms and the first-band hole pockets (see Fig. 1). The maximum period corresponding to this orbit was found by Joseph and Gordon to be $2.25\times10^{-7}$ G$^{-1}$ for $H$ in $(11\bar{2}0)$ at 28.5° to $b_3$. The minimum extremal area included in this orbit is 0.012 a.u.$^{-2}$, a factor of 10 greater than the minimum cross sectional area of the waists of the monster.

We have measured the pressure variation of an extremal area corresponding to the $P_3$ orbit to 4 kbar. The field was in $(11\bar{2}0)$ at 20° to $b_3$, or 8.5° from the orientation corresponding to the minimum extremal area. The period we measure at zero pressure is $(2.222\pm0.015)\times10^{-7}$ G$^{-1}$ in good agreement with the result of Joseph and Gordon for this orientation. The rate of change of the diagonal-arm area with pressure is

$$d\ \ln S_3/dP=-(1.27\pm0.07)\times10^{-2}\ (\text{kbar})^{-1}. \quad (22)$$

In contrast with the needle and waist sections of the FS, the diagonal arms of the combined 1st- and 2nd-band hole surface become thinner with increasing pressure. No attempt was made to measure $d\ \ln m_3^*/dP$.

### B. Comparison of the $P_3$ Pressure Results with the NFEM and with the Alloy Results

The 1-OPW minimum extremal cross sectional area for the diagonal arms is 0.017 a.u.$^{-2}$, in good agreement with the observed value of 0.012 a.u.$^{-2}$. The minimum NFEM cross-sectional area was determined for $H$ at 28.5° to $b_3$ in $(10\bar{1}0)$. A triangular segment which

TABLE I. Experimental results for the effect of pressure on the three sections of the Zn Fermi surface studied in this work. The associated model predictions are enclosed in brackets. [Units are $10^{-3}$ (kbar)$^{-1}$.]

| Fermi surface section | $d\ln S_i/dP$ | $d\ln m_i^*/dP$ |
|---|---|---|
| Needles ($S_1$) | $32 \pm 1.5$ [13 (NFEM)] | $14\pm2$[16 (NFEM with experimental $d\ln S_1/dP$)] |
| Waists ($S_2$) | $3.94\pm0.10$ [2.8 (Modified NFEM); 2.2 (3-OPW)] | $<\pm2$[$\cong$1.5 (Modified NFEM)] |
| Diagonal arms ($S_3$) | $-1.27\pm0.07$[$-0.8$ (NFEM)] | |

approximated the 1-OPW area to within about 15% was chosen and the relative change in area of this segment with pressure was determined using the measured linear compressibilities at 4.2°K.[28] No correction was made for the difference between the 1-OPW and observed areas at zero pressure. The NFEM prediction for the relative pressure coefficient of the diagonal-arm area is

$$d\ln S_3(\text{NFEM})/dP = -0.8\times10^{-2}\ (\text{kbar})^{-1}. \quad (23)$$

The NFEM correctly predicts the sign of the pressure effect on the diagonal arms and the actual numerical agreement is comparable with that between the NFEM prediction and the observed pressure dependence of the waist section. Using the above approximation and the values for the change in the lattice parameters with alloying used by Higgins and Marcus, we estimate that the NFEM prediction is within the scatter of $\pm1\%$ that Higgins and Marcus assigned to the comparison between the period measurements of $P_3$ in 0.21% Zn-Cu and pure Zn. The enhanced effect of alloying apparent in the waist results is not apparent in the $P_3$ alloy results.

## VI. SUMMARY

The minimum cross-sectional area of the needles in Zn increases by nearly 100% with a pressure of 3 kbar. From a comparison between the pressure change of the needle area measured with solid He and with gaseous He as pressure transmitting media, we conclude that the solid-He technique assures hydrostatic conditions even at relatively low pressures (1 kbar) and for materials with highly anisotropic thermal expansitivities. Earlier results[10,11] for the change of the dHvA period and mass of the needles under uniform compression are spurious. In these measurements it was assumed that the ice-bomb technique yielded hydrostatic-pressure conditions. This assumption is certainly invalid in the case of Zn. There is a factor of two disagreement between our result for the needle pressure change and the $(\Delta\rho_{11}/\rho_0)_{\text{osc}}$ results of Gaidukov and Itskevich[12] who used the frozen oil-kerosene technique to generate pressure. This technique is much improved over the ice-bomb method but does not provide a hydrostatic-pressure environment in the case of Zn for pressures of 7 kbar or below. Later results of Itskevich, Voronovskii, and Sukhoparov[31] suggest that at higher pressures the frozen oil-kerosene medium probably flows enough to achieve more nearly hydrostatic conditions.

Our experimental results and the relevant model predictions are summarized in Table I. In general, we find that the NFEM gives a qualitatively correct estimate of the pressure effect on the three sections of the Zn FS investigated. For $H\|b_3$, the NFEM underestimates the rate of increase of the needle area with pressure by a factor of 2. Since the NFEM estimate depends very sensitively upon the initial value of the $c/a$ ratio, this difference is of doubtful significance. The agreement between $d\ln S_1/d[Z/(c/a)]$ determined from the Zn-Cu alloy measurements[15] and $-[d\ln S_1/d(c/a)]_Z$ determined from this pressure study supports the conclusion that the NFEM expression correctly accounts for the dependence of the area upon $Z/(c/a)$. The close agreement between the experimental and NFEM values for $d\ln m_1^*/dP$ is additional evidence that the needle sections of the Zn FS are highly free-electron-like. A modified NFEM approximation ($k_F$ increased by about 3%) to the waists of the monster gives an agreement to within 50% with the experimental pressure effect. The same model underestimated the area changes due to alloying by a factor of 4. The results of a model pseudopotential calculation of the changes in the minimum-waist area due to pressure and alloying leave the relative discrepancy between the pressure and alloy results and theory unchanged. The larger difference between the model predictions and the observed changes of the waist area with alloying is not understood. The possibility that the discrepancies result from large uncertainties in the change of the lattice parameters with alloying would seem to be ruled out by the excellent agreement between the alloy and pressure results for the needles. The model pseudopotential used gives a poor fit to the form factor $W(002)$. The calculation must be repeated using a better model potential before the relative agreement of the NFEM and 3-OPW predictions to the waist pressure results can be considered significant. The NFEM correctly predicts the sign of the pressure effect on the diagonal arms of the monster. A comparison between the relative fit of the pressure and alloy results to the NFEM is not possible, because no significant alloying effect on $P_3$ was observed by Higgins and Marcus.

## ACKNOWLEDGMENTS

The authors have benefited from a number of helpful conversations with Professor W. L. Gordon, Professor R. J. Higgins, and Professor J. R. Anderson. L. Bru-

baker and D. Sand contributed valuable technical assistance throughout this work.

## APPENDIX

We consider a simplified description of the audio-modulation method in the low-frequency region where the ac skin depth is greater than the sample radius. We assume: (1) a geometry consisting of an infinitely long cylindrical sample of radius $a$; (2) an applied field directed along the sample axis, consisting of a steady component $H_0$ and an oscillatory component $h_0\cos\omega t$ with *small* $h_0(h_0\ll H_0)$; (3) the oscillatory magnetization, $M_{\rm osc}$, is parallel to the cylinder axis and both $M_{\rm osc}$ and $\sigma_{\rm osc}$ (the oscillatory conductivity) are *linear* functions of the magnetic field. These assumptions can be reasonably well satisfied in the case of the Zn needles for $H\|b_3$ and $h_0$ much less than the separation in applied field between two neighboring oscillations. We wish to determine an estimate of the relative importance of the oscillatory magnetic and conductivity contributions[46] to the emf across a pickup coil surrounding the sample. This question is significant in the case of the Zn needle oscillations where there are large amplitude oscillations in the magnetoresistance as well as in the susceptibility.

The field in the cylinder satisfies the equation,

$$\nabla^2H+(d\ln\sigma/dH)(\partial H/\partial r)^2=(4\pi\sigma/c^2)(\partial B/\partial t). \quad \text{(A1)}$$

The nonlinear term follows from the radial dependence of $\sigma$. Under our experimental conditions we estimate that,

$$(d\ln\sigma/dH)(\partial H/\partial r)^2<(0.1)\nabla^2H, \quad \text{(A2)}$$

where Stark's[17] magnetoresistance data has been used to arrive at this estimate. Following Shoenberg and Stiles[19] we set,

$$\partial B/\partial H\cong\mu_0+\lambda_0H, \quad \text{(A3)}$$

and

$$\sigma\cong\sigma_0+h(d\sigma/dH)_{H_0}\cong\sigma_0+h\sigma_0'$$

where $\mu_0=1+4\pi(dM/dH)_{H_0}$ and $\lambda_0=4\pi(d^2M/dH^2)_{H_0}$. If we neglect the nonlinear term in Eq. (A1) and insert the approximate forms, Eq. (A3), Eq. (A1) can be written

$$\nabla^2h=(4\pi\sigma_0\mu_0/c^2)(1+\gamma h)\partial h/\partial t, \quad \text{(A4)}$$

where $\gamma=(\lambda_0/\mu_0)+(\sigma_0'/\sigma_0)$. We look for a harmonic solution of the form

$$h\cong R\{h_1e^{i\omega t}+h_2e^{i2\omega t}\},$$

where $h_1$ is a solution of the homogeneous equation,

$$\nabla^2h_1+k^2h_1=0, \quad \text{(A5)}$$

with $k^2=(1+i)\mu_0/\delta^2$ and $\delta$ (the ac skin depth) is $c/(2\pi\omega\sigma_0)^{1/2}$. The solution of Eq. (A5) consistent with the boundary conditions of our problem is,

$$h_1=R[h_0e^{i\omega t}(J_0(kr)/J_0(ka))]. \quad \text{(A6)}$$

The total first-harmonic component in the emf in a pickup coil wound about the sample is

$$E=R[(Nc^2h_0/2\sigma_0)e^{i\omega t}((J_1(ka)/J_0(ka))]. \quad \text{(A7)}$$

In the low-frequency limit ($|ka|<1$) the Bessel functions can be expanded in a power series in $(ka)$. The first-order contribution to the net emf (the difference between the emf with and without the sample) is simply,

$$E_{1,\,\rm net}=-4\pi N(\pi a^2)(dM/dH)_{H_0}\partial h/\partial t. \quad \text{(A8)}$$

The relative magnitude of the second- and first-order contribution is given by

$$|E_{2,\,\rm net}|/|E_{1,\,\rm net}|\cong\tfrac{1}{2}(a/\delta)^2. \quad \text{(A9)}$$

Thus in the limit as $a/\delta$ becomes much less than 1, and for small modulation amplitude, the first harmonic contribution to the net emf is due entirely to the susceptibility. In the case of our Zn samples the ratio of $|E_2|/|E_1|$ is about $10^{-2}$ for $\omega/2\pi\cong6$ cps.

The determination of the complete solution to Eq. (A4) is not straightforward as it is in the strictly one-dimensional case considered by Shoenberg and Stiles.[19] However, it is possible to see by inspection that the relative conductivity and susceptibility contribution to the second-harmonic signal is roughly determined by the ratio of $(\sigma_0'/\sigma_0)$ to $(\lambda_0/\mu_0)$. From this we would conclude that there should be an important contribution from $(\Delta\rho/\rho_0)_{\rm osc}$ to our 2nd-harmonic needle-oscillation data.

[46] This problem has been examined independently by S. J. Williamson (private communication).